Proceedings of the 2009 IEEE International Conference on Systems, Man, and Cybernetics
San Antonio, TX, USA - October 2009

Motion Analysis by Experiment and Simulation for Riding Bicycles with Children

Shunsuke MATSUZAWA
Department of Robotics and Mechatronics
Tokyo Denki University
2-2, Nishiki-cho, Kanda, Chiyodas-ku, Tokyo, Japan
matuzawa@hatalab.k.dendai.ac.jp

Masami IWASE, Teruyoshi SADAHIRO,
Shoshiro, HATAKEYAMA
Department of Robotics and Mechatronics
Tokyo Denki University
2-2, Nishiki-cho, Kanda, Chiyodas-ku, Tokyo, Japan
{iwase, sadahiro, sho}@fr.dendai.ac.jp

***Abstract*—The purpose of this paper is motion analysis by experiment and simulation for riding bicycles with children. It is very important to think about stability when the bicycle is driving with children. However, such a research is not so performed. Therefore, analysing human motions in the such case by some experiments and simulations, dynamic characteristics of the such case are shown. The modeling of bicycle is performed, and the model is used for the simulations.**

***Index Terms*—riding bicycles with children, motion analysis, modeling**

I. Introduction

An automobile is one of the most familiar vehicle. In the recent years, the automobile has a lot of problems such as the greenhouse gases caused by automobiles, the cost of fuel up and so on. In this situation, riding a bicycle attracts attentions again as a no-emission vehicle. The bicycle also has many advantages such as keeping and increasing rider's health, relief of traffic congestion and energy efficiency. However, since the bicycle is an unstable system, a certain amount of skill is needed to perform stable riding. Many study on two-wheeled vehicles such as bicycles and electric motorbikes have been done[1][2]. Saguchi has realized stable running on straight-line and curve motions using a model which is considered the skid of the wheels[3]. Satou has realized stabilizing a bicycle to control a handle and center of gravity(COG) by an attached cart-mass system[4].

The law concerning the safety on the riding bicycle with two-children is examinated in July 2008, in Japan. If the conditions such as stability, rigidity, braking characteristics and vibration, does not spoiled when a riding bicycle with two children ,it is allowed by the law. However, the clear numerical standards in such case are not shown yet.

In this research, in order to consider the stability of the bicycle when riding with small children on a bicycle and driving, some experiments are conducted. Using the results, to develop an assistance-system for riding bicycle with two-children is our final research objective. In this paper, an experimental system to measure states of a bicycle is built in order to dedicate developing the such system. A state is analyzed to establish some safety standards to the riding bicycle with two-children when the weight assumed as small children is put on infant seats. In order to verify the results in the numerically, the modeling of the bicycle on three-dimensional space is performed.

II. Experimental system.

An experimental system uses an inertial sensor which can measure the angle of three axes of the main part of a bicycle, angular velocity, and acceleration, a gyro sensor which can measure the angular velocity of a handle and a cycle sensor for measuring the number of rotations of a rear wheel of a bicycle. The specification of the inertial sensor and the gyrosensor are shown in Tab.I, an inertial sensor is shown in Fig.1, the gyro sensor is shown in Fig.2, the cycle sensor is shown in Fig.3 and an attachment position of the inertial sensor and its coordinates are shown in Fig.4.

TABLE I
The specification of the inertial sensor and the gyro sensor.

Sensor name.	Inertial sensor.	Gyro sensor.
Angle.[deg]X Z,Y	$\pm 180, \pm 90$	
Angular velocity.[deg/sec]	± 100	± 573
Acceleration.[G]	± 4	
Outside.[mm]	$76.2 \times 95.3 \times 104.2$	$27.0 \times 27.0 \times 10.2$

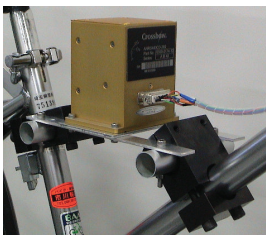

Fig. 1. Inertial sensor.

Fig. 2. Gyro sensor.

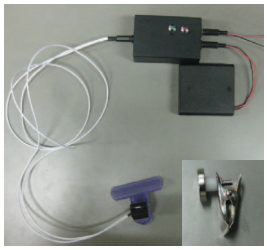

Fig. 3. Cycle sensor.

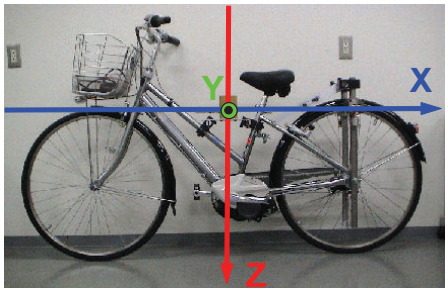

Fig. 4. The attachment position of the inertial sensor and its coordinates.

An origin of the bicycle coordinates is the center of the inertial sensor. The X-axis is set as the counter direction of proceeding, the Z-axis is set as perpendicular downward to the ground and the Y-axis is set as the left when turning to the direction of proceeding as shown in Fig.4. The gyro sensor attached to the handle is set a clockwise rotation positive. The cycle sensor is attached to the rear wheel of the bicycle, and acquires the degree of rotation angle of the rear wheel.

III. A MEASUREMENT EXPERIMENT OF THE BICYCLE WHICH CARRIED WEIGHT.

Three experiments, which are consisted by straight, meandering and the circumference are held. We conside four conditions for the weight condition, that are front and rear(both), front only, rear only and nothing. Measurement is performed two times for each conditions. Other detailed experimental conditions are shown in Tab.II. The conditions for riding meandering is shown in Fig.5. The conditions for riding circumference is shown in Fig.6.

TABLE II
EXPERIMENTAL CONDITION.

The number of volunteer.	4age
Weight of volunteer A and D.	30[kg]
Weight of volunteer B and C.	20[kg]
Measurement time.	20[sec]
The interval of meandering(Width).	6[m]
The interval of meandering(Length).	6.9[m]
The radius of the circumference.	3[m]

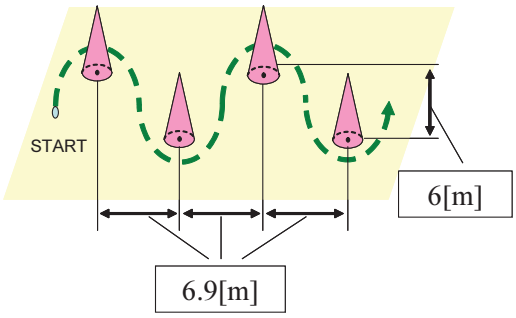

Fig. 5. The conditions for riding meandering.

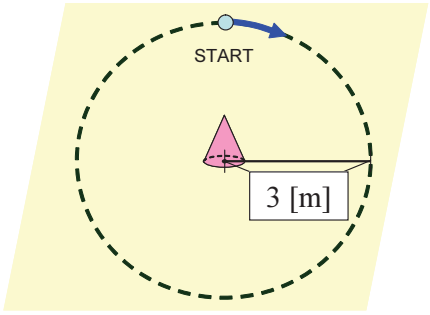

Fig. 6. The conditions for riding circumference.

The weight of the experiments are used max one that each volunteer can ride the bicycle, because to mimic the realistic situation that is needed to ride a bicycle with two-children, our volunteers are more powerful and younger than situation.

IV. EXPERIMENTAL RESULTS

Due to the page limitation, in this paper, the results compared with the weight is only rear and nothing, that is shown big defferences, are shown. The comparison waveform of the angle of the X-axis of going straight of volunteers A, B, C, and D is shown in Fig.7, Fig.8, Fig.9 and Fig.10 when the weight is only rear and nothing.

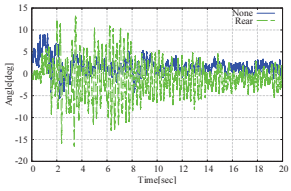

Fig. 7. Angle on riding straight of volunteer A.

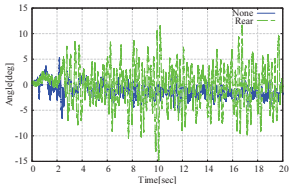

Fig. 8. Angle on riding straight of volunteer B.

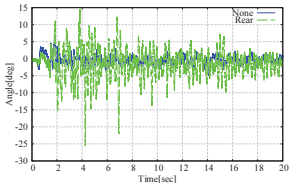

Fig. 9. Angle on riding straight of volunteer C.

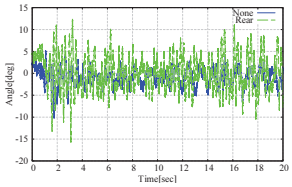

Fig. 10. Angle on riding straight of volunteer D.

The solid line of Fig.7, Fig.8, Fig.7 and Fig.8 is when the weight is nothing, and the dashed line is waveform when weight is rear only. To compare with four waveforms, the waveform when the weight is rear only has big amplitude than the waveform when weight is nothing. Due to the page limitation, in this paper, the comparison waveform of two weight positions which is nothing and rear only is shown. However, it is checked that these results are the features which appear irrespective of the weight positions.

These measurement waveforms using FFT is shown in Fig.11, Fig.12, Fig.13, and Fig.14.

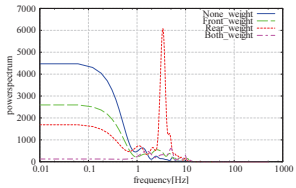

Fig. 11. FFT of volunteer A angle

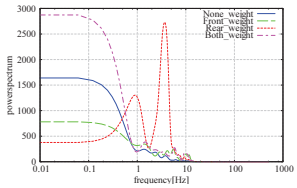

Fig. 12. FFT of volunteer B angle

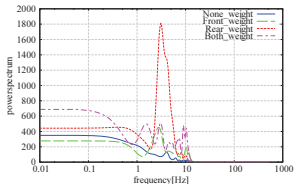

Fig. 13. FFT of volunteer C angle

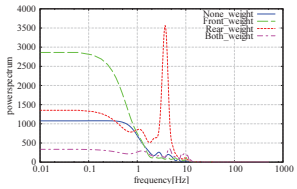

Fig. 14. FFT of volunteer D angle

In these figures, the solid line means the result of the weight is nothing, the dashed line means front only, the dotted line means rear only and the dotted and dashed line means both. From the results of FFT, frequency of per 3 - 4[Hz] on the weight is rear only is large for all volunteers. When the weight is nothing, front only and both, amount of low frequency waves has increased.

The variances of the obtained angles are shown in Fig.15, Fig.16 and Fig.17.

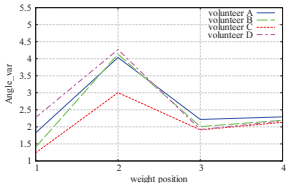

Fig. 15. Variances of the angles on riding straight.

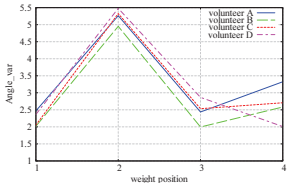

Fig. 16. Variances of the angles on riding meandering.

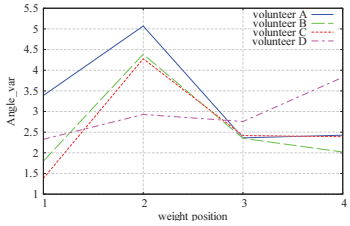

Fig. 17. Variances of the angles on riding circumference.

A horizontal axis show variance of the X axial angle of the bicycle, and a vertical axis show the weight position. The solid line is volunteer A, the dashed line is volunteer B, the dotted line is volunteer C and the dotted and dashed line is volunteer D. In Fig.15, it is shown that the variances when weight is rear only is large every volunteer on riding straight. In Fig.16 and Fig.17, it is shown also that the variances when weight is rear only is large every volunteer on riding meandering and circumference.

These results showed that the weight is rear only becomes very unstable irrespective of a volunteer and riding conditions.

It is necessary to confirm whether a similar tendency appears in not only experimental but also the numerically. To devise the method of guaranteeing stability that the model is needed. Therefor, modeling of the bicycle is perform.

V. Modeling of the Bicycle on Three-Dimensional Space

Model is needed in order to check experimental results. Model is also needed in order to perform stability analysis and construction of a support system using simulations.

The modeling of the bicycle in three-dimensional space is performed using the Projection Method. The Projection Method is a modeling method to consider model's constraint. In complex models, it is difficult to consider the constraints, but it is easy to derive the motion equation using other, e.g. Lagrange Method, modeling method. In the Projection Method, positional constraint is one of the easiest constraint to consider, so the weight is not taken into consideration in this paper, because it is easy to attach.

To derive a model of a bicycle, we assume that the equation of the motion of the wheel on the two-dimensional plane has already derived by the Projection Method[6]. Fixing the two wheels and the handle by appropriate constraint conditions that

are not easy to derive, the equation of the motion of the bicycle is derived by the Projection Method. Due to the page limitation, in this paper, the details of modeling are excluded. A detailed modeling result is shown in [6] of bibliography.

A. The outline of the modeling by the Projection Method.

The Projection Method is performed as the following procedures.

1) A model diagram of modeled mass system is illastlated and its coordinate system is defined.
2) The character and number showing physical parameters, such as a center-of-gravity position of a mass point and length, are assigned..
3) Sufficient parameter required to express this system is defined as a generalized coordinate q_a.
4) Generalization velocity is defined corresponding to a generalized coordinate.
5) In order to derive the equation of motion in the state where it is not constrainted, the equation of motion is derived for each element of a generalized coordinate.The generalization mass matrix M, the generalization force matrix h and the generalized velocity v are decided gathring up the matrix form as ($M\dot{v} = h$).
6) The constraint conditions imposed on this system are enumerated.
7) From constraint conditions, the constraint matrix C satisfies $Cv = 0$ is derived.
8) The equation of motion with constrainted reaction forces are described as $M\dot{v} = h + C^T\lambda$ using Lagurange multiplier λ.
9) The independent velocity $\dot{q}$ after the system was constrained.
10) The orthogonal matrix D which satisfies ($CD = 0$) and ($v = D\dot{q}$) is derived.
11) The equation of motion being constrainted is projected on the space which makes the column vector of D a base vector.The equation of motion of only the flexibility after being constrainted is obtained by carrying out coordinates conversion of the ingredient vector.

$$\left(D^T M D\ddot{q} + D^T M \dot{D}\dot{q} = D^T h\right)$$

A model figure, the Projection Method of a parameter and the constraint conditions which become important in the modeling of the bicycle in 3-dimensional space are shown below.

B. A model figure and the account method of a parameter.

The model of the bicycle is shown in Fig.18 and Fig.19. Parameters of the bicycle is shown in Tab.III.

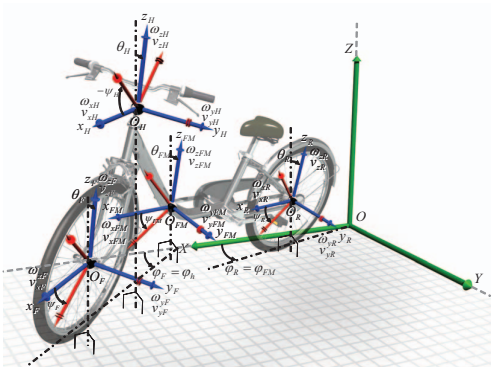

Fig. 18. A bicycle model and its coordinate systems and parameters on 3D-space.

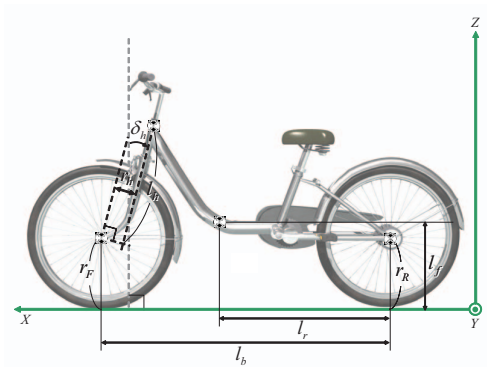

Fig. 19. A bicycle model and its coordinate systems and parameters on the lateral plane.

TABLE III
THE PARAMETER DEFINITION

Mass of the front wheel	m_F[kg]	1.5
Radius of the front wheel	r_F[m]	0.33
Mass of the rear wheel	m_R[kg]	1.5
Radius of the rear wheel	r_R[m]	0.33
Wheelbase	l_b[m]	1.07
Mass of the handle	m_H[kg]	1.0
Length of the front fork	l_h[m]	0.55
Angle of the front fork	δ_h[m]	20.0
Offset of the front wheel	r_h[m]	0.06
Mass of the frame	m_{FM}[kg]	16.0
Length from the rear wheel to the frame	l_b[m]	1.07
Height of the frame	l_f[m]	0.5
Inertia moment of the front wheel about x_F, z_F axis	I_{xzF} [kg · m^2]	0.04
Inertia moment of the front wheel about y_F axis	I_{yF} [kg · m^2]	0.08
Inertia moment of the rear wheel about x_R, z_R axis	I_{xzR} [kg · m^2]	0.04
Inertia moment of the rear wheel about y_R axis	I_{yR} [kg · m^2]	0.08
Inertia moment of the handle about x_H, z_H axis	I_{xzH} [kg · m^2]	0.01
Inertia moment of the handle about y_H axis	I_{yH} [kg · m^2]	0.01
Inertia moment of the frame about x_{FM}, z_{FM} axis	I_{xzFM} [kg · m^2]	0.81
Inertia moment of the frame about y_{FM} axis	I_{yFM} [kg · m^2]	1.62

C. The constraint condition.

The constraint conditions between the front wheel and the rear wheel are held as follows:

- The relation between the arc by the front wheel and the arc by the rear wheel is

$$r_F\psi_F \cos(\phi_F - \phi_R) = r_R\psi_R. \quad (1)$$

- The relation between the arc by the front wheel and the track by the rear wheel is

$$r_F \psi_F \sin(\phi_F - \phi_R) = l_b \phi_R. \tag{2}$$

- The relation between inclination of the front wheel and the rear wheel is

$$r_R \omega_{xR} \cos\theta_R = r_F \omega_{xF} \cos\theta_F \cos(\phi_F - \phi_R). \tag{3}$$

The constraint conditions between the front wheel and the handle are held as follows:

- The positional constraint that the handle is connected to the front wheel is

$$\boldsymbol{x}_H = R_z(\phi_H) R_x(\theta_H) R_y(\psi_H) \begin{bmatrix} -r_h \\ 0 \\ l_h \end{bmatrix} + \boldsymbol{x}_F, \tag{4}$$

where $\boldsymbol{x}_F = \begin{bmatrix} x_F & y_F & z_F \end{bmatrix}^T$ is the vector of COG of the front wheel and, $\boldsymbol{x}_H = \begin{bmatrix} x_H & y_H & z_H \end{bmatrix}^T$ is the vector of COG of the handle. The rotation matrix $R_z(\phi_H), R_x(\theta_H), R_y(\psi_H)$ are represented as

$$R_z(\phi_H) = \begin{bmatrix} \cos\phi_H & -\sin\phi_H & 0 \\ \sin\phi_H & \cos\phi_H & 0 \\ 0 & 0 & 1 \end{bmatrix}, \tag{5}$$

$$R_x(\theta_H) = \begin{bmatrix} 1 & 0 & 0 \\ 0 & \cos\theta_H & -\sin\theta_H \\ 0 & \sin\theta_H & \cos\theta_H \end{bmatrix}, \tag{6}$$

$$R_y(\psi_H) = \begin{bmatrix} \cos\psi_H & 0 & \sin\psi_H \\ 0 & 1 & 0 \\ -\sin\psi_H & 0 & \cos\psi_H \end{bmatrix}. \tag{7}$$

- The relation between the angle of inclination of the front wheel and the angle of inclination of the handle, and the relation between the steering angle of the front wheel and the steering angle of the handle are

$$\theta_F = \theta_H, \tag{8}$$

$$\phi_F = \phi_H. \tag{9}$$

- The relation between the front fork angle and the handle angle is

$$\psi_H = -\delta_h. \tag{10}$$

The constraint conditions between the rear wheel and the frame are held as follows:

- The positional constraint that the frame is connected to the rear wheel is

$$\boldsymbol{x}_{FM} = R_z(\phi_{FM}) R_x(\theta_{FM}) R_y(\psi_{FM}) \begin{bmatrix} l_r \\ 0 \\ l_f - r_R \end{bmatrix} + \boldsymbol{x}_R, \tag{11}$$

where $\boldsymbol{x}_R = \begin{bmatrix} x_R & y_R & z_R \end{bmatrix}^T$ is the vector of COG of the rear wheel and, $\boldsymbol{x}_{FM} = \begin{bmatrix} x_{FM} & y_{FM} & z_{FM} \end{bmatrix}^T$ is the vector of COG of the frame. The rotation matrix $R_z(\phi_{FM}),\ R_x(\theta_{FM}),\ R_y(\psi_{FM})$ are represented as

$$R_z(\phi_{FM}) = \begin{bmatrix} \cos\phi_{FM} & -\sin\phi_{FM} & 0 \\ \sin\phi_{FM} & \cos\phi_{FM} & 0 \\ 0 & 0 & 1 \end{bmatrix}, \tag{12}$$

$$R_x(\theta_{FM}) = \begin{bmatrix} 1 & 0 & 0 \\ 0 & \cos\theta_{FM} & -\sin\theta_{FM} \\ 0 & \sin\theta_{FM} & \cos\theta_{FM} \end{bmatrix}, \tag{13}$$

$$R_y(\psi_{FM}) = \begin{bmatrix} \cos\psi_{FM} & 0 & \sin\psi_{FM} \\ 0 & 1 & 0 \\ -\sin\psi_{FM} & 0 & \cos\psi_{FM} \end{bmatrix}. \tag{14}$$

- The relation between the angle of inclination of the rear wheel and the angle of inclination of the frame, and the relation between the steering angle of the rear wheel and the steering angle of the frame are

$$\theta_R = \theta_{FM}, \tag{15}$$

$$\phi_R = \phi_{FM}. \tag{16}$$

- The relation of the pitch angle of the frame is

$$\psi_{FM} = 0. \tag{17}$$

The constraint matrix C is drawn using these constraint conditions.

D. Dynamical system with constraints.

The equation of motion after being constrainted using constraint matrix C, the generalization power matrix h, the generalization mass matrix M and the differentiation of general acceleration $\ddot{v}$ is

$$M_a \dot{\boldsymbol{v}}_a = \boldsymbol{h}_a + C_a^T \lambda, \tag{18}$$

where λ is a Lagrange undecided multiplier. The equation of motion of the bicycle when a Lagrange undecided multiplier is eliminated from an Eq.(1) using the orthogonal matrix is

$$D_a^T M_a D_a \ddot{\boldsymbol{q}} + D_a^T M_a \dot{D}_a \dot{\boldsymbol{q}} = D_a^T \boldsymbol{h}_a.$$

VI. Model verification

The nonlinear model that is derived in the previous section is verified to compare with behaviors of the real system and numerical simulations using it.The initial velocity of the rear wheel is $0.0\ [rad/s]$. Trajectories of the steering angle ϕ_h and the inclination angle of the frame θ_{FM} are shown in Fig.20. Initial velocity of the rear wheel is $0.0\ [rad/s]$ and initial inclination of the frame is $0\ [deg]$.

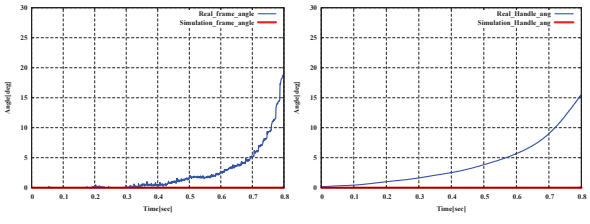

Fig. 20. Trajectories of the steering angle ϕ_h and the inclination angle of the frame θ_{FM} when the initial inclination of the frame is set to 0 $[deg]$.

From Fig.20, It is shown that the steering angle and the inclination angle of the real system and these of the nonlinear model are not same. Because it is difficult to set the initial steering angle of the real system at $\phi_h = 0$, in fact, the initial steering angle is 0.4 $[deg]$. Therefore, we simulate two cases. One is the initial steering angle is set to 0.4 $[deg]$, and the other one is the initial steering angle is set to 30 $[deg]$. The results are shown in Fig.21 and Fig.22.

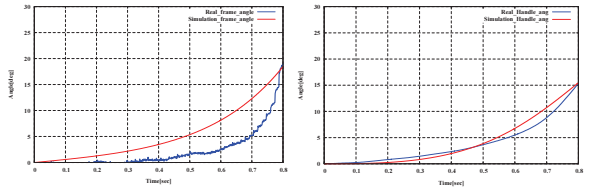

Fig. 21. Trajectories of the inclination angle of the frame θ_{FM} and the steering angle ϕ_h when the initial inclination of the frame is set to 0.4 $[deg]$.

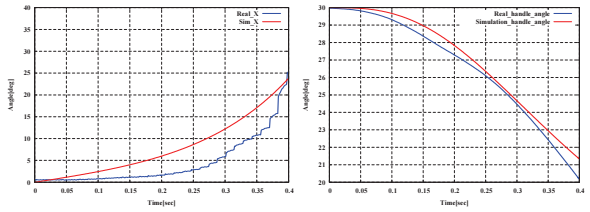

Fig. 22. Trajectories of the inclination angle of the frame θ_{FM} and the steering angle ϕ_h when the initial inclination of the frame is set to 30 $[deg]$.

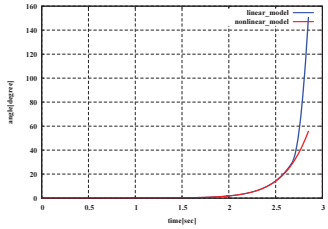

Fig. 23. The trajectorys of the inclination angle of the frame for the proposed nonlinear model and the linear model.

From Fig.21, the handle rotates towards the angle which the frame is inclined when the frame is inclined. From Fig.22, the handle rotates towards the angle which the frame is not inclined when the frame is inclined. From Fig.21, and Fig.22, the behaviors of the proposed nonlinear model is similar to the real system.

To show the validity of the proposed nonlinear model, it is compared with the linear model by the simulation. The trajectories of the inclination angle of the frame for both models is shown in Fig.23. From Fig.23, it is clearly shown that the inclination angle of the linear model is differ from the angle of the nonlinear model after $\theta_{FM} = 30$ $[deg]$, so the conventional linear models is not so useful to consider stablizing the bicycle in the wide inclination angles. Therefore, the nonlinear model is very important to develop a stable bicycle riding support system and analyze the stability of the bicycle under various situations.

VII. Conclusion

In this paper, the experimental system to measure stability of the riding bicycle with two children was constructed. The stability of the riding bicycle with weights which assumed to children was measured by the experimental system. The difference between presence of weight and driving condition were compared and analyzed using the result. The modeling of the bicycle which is needed in order to perform verification of an experimental result, analyze the stability and construct the support system using a simulation was performed.

In the future, I will increase the number of experiments samples and measure the stability of the riding bicycle with children. And, verify the analytical result using the motion equation of the derived three dimension space. From the result in becoming unstable when the bicycle rear is heavy, I develop the support system to the handle of the riding bicycle with children.

References

[1] Åström,K.J, Klein,R.E, Lennartsson,A, "Bicycle dynamics and control", Control Systems Magazine, IEEE, Volume 25, pp. 26-pp. 47, 2005

[2] Ko Iuchi, Hiroshi Niki and Toshiyuki Murakami, "Attitude Control of Bicycle Motion by Steering Angle and Variable COG Control", *IECON2005*, 2005

[3] SAGUCHI Taichi, YOSHIDA Kazuo, TAKAHASHI Masaki, "Stable Running Control of Autonomous Bicycle Robot", Transactions of the Japan Society of Mechanical Engineers. C 2006, 2006

[4] Takushi Satou, Tohru Namekawa, "Robust running stabilization of an independence running two-wheeled vehicle to change of speed and mass", The Society of Instrument and Control Engineers, Volume42, No. 1 1/8, 2006

[5] W. Arczewski, W.Blajer, " A Unified Approach to the Modelling of Holonomic and Nonholonomic Mechanical Systems ", Mathematical Modelling of Systems, Vol. 2, No. 3, pp157-pp174, 1996

[6] Hiroshi Ohsaki, Masami Iwase, Shoshiro Hatakeyama, "A Consideration of Nonlinear System Modeling using the Projection Method", SICE Annual Conference 2007, 2007

[7] Hirokazu Ohno, Shunsuke Matsuzawa and Mawami Iwase, "MODELING AND ANALYSIS OF A BICYCLE ON THE THREE-DIMENSIONAL SPACE USING THE PROJECTION METHOD", 6th Vienna International Conference on Mathematical Modelling, 2009